International Journal of Solids and Structures 45 (2008) 5381–5396

Contents lists available at ScienceDirect

International Journal of Solids and Structures

journal homepage: www.elsevier.com/locate/ijsolstr

Analysis of fatigue delamination growth for piezoelectric laminated cylindrical shell considering nonlinear contact effect ☆

Zhu Fuhui *, Fu Yiming, Chen Deliang

College of Mechanics and Aerospace, Hunan University, Changsha 410082, China

A R T I C L E I N F O

Article history:
Received 12 January 2008
Received in revised form 1 April 2008
Available online 10 June 2008

Keywords:
Piezoelectric laminated cylindrical shells
Energy release rate
Fatigue delamination growth
Nonlinear contact effect

A B S T R A C T

This paper presents a nonlinear analysis model of fatigue delamination growth for piezoelectric laminated cylindrical shells with asymmetric laminations. Considering the geometric nonlinearity and the nonlinear contact effect, the nonlinear governing equations and corresponding matching conditions for the delaminated shells are established by using the movable-boundary variational principle. According to the Griffith criterion and Paris law, the energy release rate and delamination growth rate along the delamination front are determined. Then, using cyclic skip method, the delamination growth lengths are derived. In numerical examples, the effects of the voltages, stiffness factor of contact region, asymmetry of delamination and delamination length on energy rate and delamination growth length are discussed.

1. Introduction

Composite laminates have been widely used in engineering on account of their excellent properties, such as high strength-to-weight ratio, high stiffness-to-weight ratio and designability. However, the delamination damage will easily emerge in composite laminates during the manufactures and in-service life. What's more, the great stress concentration along the delamination front may cause the delamination growth in delaminated composite structure under the action of cyclic load and finally result in the failure of structure. Since the composite laminated cylindrical shells are the significant structures utilized in the aerospace and military engineering, the research on the fatigue delamination growth of piezoelectric delaminated laminated cylindrical shells receives more and more attention.

Up to now, many researchers paid concentrations on the discussion of the thin-film delamination and the analysis of delamination growth for beam-plates. But few investigations have been reported on the fatigue delamination growth for piezoelectric laminated cylindrical shells. The evolution of the crack growth speed in a buckled one-dimensional delamination model was studied and two approximate solutions were presented by Yin (1993). Applying Mindlin nonlinear plate theory, the dynamic problems of the plates with irregular delamination were analyzed and the energy release rate of dynamic delamination was derived by Giannakopoulos and Nillsson (1993). The present state of studies on interfacial wave and interfacial dynamic fracture was summarized by Wang (1993) and they indicated that the new solution method was asked especially for planar transient growth. The advances of studies on the dynamic growth initiation of cracks were represented and the vital experiments and the results of them corresponding to dynamic growth initiation of cracks under impact load were introduced by Zhao (1996).The energy release rate of cylindrical shells with symmetric delamination were investigated by Yang and Fu (2006), Yang et al. (2007). It must be noted that the contact effect was not considered or only the linear spring

☆ Project supported by the National Nature Science Foundation of China (No. 10572049) and Hunan Provincial Natural Science Foundation of China (No. 08jj3008).

* Corresponding author. Tel.: +86 731 8824724.
E-mail address: zny2006@yahoo.com.cn (Z. Fuhui).

0020-7683/$ - see front matter © 2008 Elsevier Ltd. All rights reserved.
doi:10.1016/j.ijsolstr.2008.05.031

contact model was utilized in the above studies. A nonlinear anti-interpenetration constrained model to study the vibration mode of isotropic delaminated beam was established by Wang (2002). Based on hump resonance principle, the effect of nonlinear contact upon natural frequency of the stiffened composite plate with pre-damages, such as delamination of skin panel and debonding interfaces between skin panel and stiffeners, is studied by utilizing the finite element method by Chen and Wang (2006).

In present study, a nonlinear analysis model of fatigue delamination growth for piezoelectric laminated cylindrical shells with asymmetric laminations is presented. Considering the geometric nonlinearity and the nonlinear contact effect, the nonlinear governing equations and corresponding matching conditions for the delaminated shells are established by using the movable-boundary variational principle (Chen, 2003; Qian, 1980; Shi, 2003). According to the Griffith criterion and Paris law, the energy release rate and delamination growth rate along the delamination front are determined. Then, using cyclic skip method, the delamination growth lengths are derived. In numerical examples, the effects of the voltages, stiffness factor of contact region, asymmetry of delamination and delamination length on energy rate and delamination growth length are discussed.

2. Basic equations

Consider a fibre-reinforced laminated cylindrical shell with two piezoelectric layers mounted on the internal and external surface as shown in Fig. 1. The shell, with throughout circumference delamination, has length L, thickness h^{e}, midsurface radius R, mass density ρ^{e} and delamination length $L^{(2)}$. In order to investigate delamination growth, the delaminated laminated cylindrical shells are divided into four regions which are respectively denoted as $\Omega^{(i)e}(i = 1–4)$. Here, signs 2, 3 represent delaminated segments, and 1, 4 represent intact segments. The lengths of regions are respectively $L^{(i)}$, and the coordinate x for each region is measured from the left end. The thickness of regions 2 is $h^{(2)e}$ and that of regions 3 is $h^{(3)e}$, obviously, $h^{(2)e} + h^{(3)\,e} = h^{e}$. In addition, there are two boundaries in the regions of delamination growth of the laminated cylindrical shells and they are written as C_j $(j = 1, 2)$, n represents the exterior normal direction of the delamination growth boundary, and δn represents the virtual delamination growth along the x direction. The piezoelectric layers with thickness h^{p} and mass density ρ^{p} are perfectly bonded on the internal and external surfaces of laminated cylindrical shells. The piezoelectric layers are denoted by $\Omega^{(i)p}$ $(i = 1–4)$. Then the whole piezoelectric laminated cylindrical shell is divided into four regions, they are denoted by $\Omega^{(i)}(i = 1–4)$, and $\Omega^{(i)} = \Omega^{(i)\,e} + \Omega^{(i)p}$.

2.1. Analysis of internal force

Supposing that $\bar{u}^{(i)}, \bar{v}^{(i)}, \bar{w}^{(i)}$ denote the displacements throughout the x, y, z direction of any points in region $\Omega^{(i)}$, and the corresponding displacement components of middle surface are $u^{(i)}, v^{(i)}$, $w^{(i)}$ respectively, the displacement components are given as

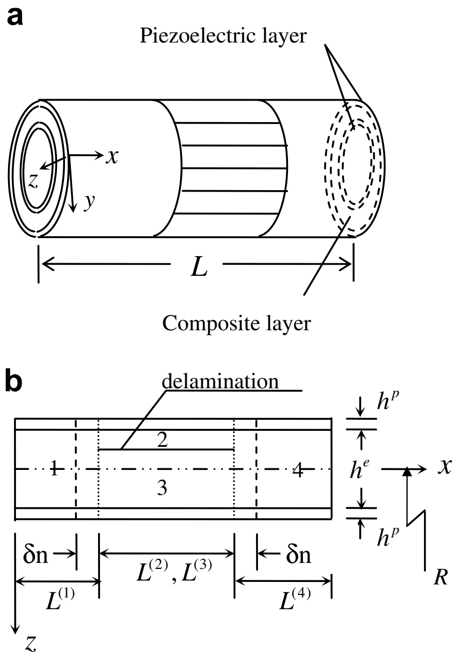

Fig. 1. (a) Geometric configuration of piezoelectric laminated cylindrical shell and (b) section of cylindrical shell.

$$\begin{aligned}\bar{u}^{(i)}(x,y,z,t) &= u^{(i)}(x,y,t) - zw^{(i)}_{,x}(x,y,t)\\ \bar{v}^{(i)}(x,y,z,t) &= v^{(i)}(x,y,t) - zw^{(i)}_{,y}(x,y,t)\\ \bar{w}^{(i)}(x,y,z,t) &= w^{(i)}(x,y,t)\end{aligned} \tag{1}$$

where a comma denotes the partial derivative with respect to the corresponding coordinate.

Assuming $\bar{\varepsilon}^{(i)}_x, \bar{\varepsilon}^{(i)}_y$ and $\bar{\varepsilon}^{(i)}_{xy}$ denote strains of any point in region $\Omega^{(i)}$, the nonlinear strain–displacement relations may be written as

$$\bar{\varepsilon}^{(i)}_x = \varepsilon^{(i)}_x + z\kappa^{(i)}_x, \quad \bar{\varepsilon}^{(i)}_y = \varepsilon^{(i)}_y + z\kappa^{(i)}_y, \quad \bar{\varepsilon}^{(i)}_{xy} = \varepsilon^{(i)}_{xy} + z\kappa^{(i)}_{xy} \tag{2}$$

where $\varepsilon^{(i)}_x, \varepsilon^{(i)}_y, \varepsilon^{(i)}_{xy}$ are the strains on the middle surface, $\kappa^{(i)}_x, \kappa^{(i)}_y, \kappa^{(i)}_{xy}$ are the change values of curvatures on the middle surface, and

$$\begin{aligned}&\varepsilon^{(i)}_x = u^{(i)}_{,x} + \frac{1}{2}w^{(i)2}_{,x}, \quad \varepsilon^{(i)}_y = v^{(i)}_{,y} - \frac{w^{(i)}}{R^{(i)}} + \frac{1}{2}w^{(i)2}_{,y}, \quad \varepsilon^{(i)}_{xy} = u^{(i)}_{,y} + v^{(i)}_{,x} + w^{(i)}_{,x}w^{(i)}_{,y}\\ &k^{(i)}_x = -w^{(i)}_{,xx}, k^{(i)}_y = -w^{(i)}_{,yy}, k^{(i)}_{xy} = -2w^{(i)}_{,xy}\end{aligned} \tag{3}$$

According to the classical theory of laminated shells, the membrane stress resultants $N^{(i)\mathrm{e}}$ and stress couples $M^{(i)\mathrm{e}}$ of the delaminated laminated cylindrical shells can be written as

$$\begin{bmatrix}[N^{(i)\mathrm{e}}]\\ [M^{(i)\mathrm{e}}]\end{bmatrix} = \begin{bmatrix}[A^{(i)\mathrm{e}}] & [B^{(i)\mathrm{e}}]\\ [B^{(i)\mathrm{e}}] & [D^{(i)\mathrm{e}}]\end{bmatrix}\begin{Bmatrix}[\varepsilon^{(i)}]\\ [\kappa^{(i)}]\end{Bmatrix} = \begin{bmatrix}[A^{(i)\mathrm{e}}_{jl}] & [B^{(i)\mathrm{e}}_{jl}]\\ [B^{(i)\mathrm{e}}_{jl}] & [D^{(i)\mathrm{e}}_{jl}]\end{bmatrix}\begin{Bmatrix}[\varepsilon^{(i)}]\\ [\kappa^{(i)}]\end{Bmatrix} \tag{4}$$

in which

$$\begin{aligned}&[N^{(i)\mathrm{e}}] = \begin{Bmatrix}N^{(i)\mathrm{e}}_x\\ N^{(i)\mathrm{e}}_y\\ N^{(i)\mathrm{e}}_{xy}\end{Bmatrix}, \quad [M^{(i)\mathrm{e}}] = \begin{Bmatrix}M^{(i)\mathrm{e}}_x\\ M^{(i)\mathrm{e}}_y\\ M^{(i)\mathrm{e}}_{xy}\end{Bmatrix}, \quad [\varepsilon^{(i)}] = \begin{Bmatrix}\varepsilon^{(i)}_x\\ \varepsilon^{(i)}_y\\ \varepsilon^{(i)}_{xy}\end{Bmatrix}, \quad [\kappa^{(i)}] = \begin{Bmatrix}\kappa^{(i)}_x\\ \kappa^{(i)}_y\\ \kappa^{(i)}_{xy}\end{Bmatrix}\\ &\qquad (A^{(i)\mathrm{e}}_{jl}, B^{(i)\mathrm{e}}_{jl}, D^{(i)\mathrm{e}}_{jl}) = \int_{-h_i/2}^{h_i/2} Q^{(k)\mathrm{e}}_{jl}(1, z, z^2)\mathrm{d}z \quad (j, l = 1, 2, 6)\end{aligned} \tag{5}$$

where $A^{(i)\mathrm{e}}_{jl}, B^{(i)\mathrm{e}}_{jl}$ and $D^{(i)\mathrm{e}}_{jl}$ are the extension, coupling and bending rigidity of laminated cylindrical shells, respectively and $Q^{(k)\mathrm{e}}_{jl}$ is elastic constant of the kth layer.

The constitutive relations of orthotropic piezoelectric layers can be described as

$$\begin{Bmatrix}\sigma^{(i)\mathrm{p}}_x\\ \sigma^{(i)\mathrm{p}}_y\\ \tau^{(i)\mathrm{p}}_{xy}\end{Bmatrix} = \begin{bmatrix}Q^p_{11} & Q^p_{12} & 0\\ Q^p_{21} & Q^p_{22} & 0\\ 0 & 0 & Q^p_{66}\end{bmatrix}\begin{Bmatrix}\bar{\varepsilon}^{(i)}_x\\ \bar{\varepsilon}^{(i)}_y\\ \bar{\gamma}^{(i)}_{xy}\end{Bmatrix} - \begin{bmatrix}0 & 0 & e_{31}\\ 0 & 0 & e_{32}\\ 0 & 0 & 0\end{bmatrix}\begin{Bmatrix}E^{(i)}_x\\ E^{(i)}_y\\ E^{(i)}_z\end{Bmatrix} \tag{6}$$

$$[D^{*(i)}] = \begin{Bmatrix}D^{*(i)}_x\\ D^{*(i)}_y\\ D^{*(i)}_z\end{Bmatrix} = \begin{bmatrix}0 & 0 & 0\\ 0 & 0 & 0\\ e_{31} & e_{32} & 0\end{bmatrix}\begin{Bmatrix}\bar{\varepsilon}^{(i)}_x\\ \bar{\varepsilon}^{(i)}_y\\ \bar{\gamma}^{(i)}_{xy}\end{Bmatrix} + \begin{bmatrix}\varepsilon^*_{11} & 0 & 0\\ 0 & \varepsilon^*_{22} & 0\\ 0 & 0 & \varepsilon^*_{33}\end{bmatrix}\begin{Bmatrix}E^{(i)}_x\\ E^{(i)}_y\\ E^{(i)}_z\end{Bmatrix} = [e][\bar{\varepsilon}^{(i)}] + [\varepsilon^*][E^{(i)}] \tag{7}$$

where $\sigma^{(i)\mathrm{p}}_x, \sigma^{(i)\mathrm{p}}_y, \tau^{(i)\mathrm{p}}_{xy}$ are the stress components of piezoelectric layer, $D^{*(i)}_x, D^{*(i)}_y, D^{*(i)}_z$ are electric displacement components, $E^{(i)}_x, E^{(i)}_y, E^{(i)}_z$ are electric-field intensity components, Q^p_{ij} is elastic constant, e_{ij} is piezoelectric stress constant, and $\varepsilon^*_{11}, \varepsilon^*_{22}, \varepsilon^*_{33}$ are dielectric constants. The piezoelectric strain constant d_{ij} is commonly appointed, and the relations between e_{ij} and d_{ij} are

$$\begin{aligned}e_{31} &= d_{31}Q^{\mathrm{p}}_{11} + d_{32}Q^{\mathrm{p}}_{12}\\ e_{32} &= d_{31}Q^{\mathrm{p}}_{12} + d_{32}Q^{\mathrm{p}}_{22}\end{aligned} \tag{8}$$

Supposing only the electric-field component $E^{(i)}_z$ is applied on the piezoelectric layers throughout the thickness direction. Denoting $V^{(i)}_{\mathrm{T}}, V^{(i)}_{\mathrm{B}}$ and $E^{(i)}_{\mathrm{T}}, E^{(i)}_{\mathrm{B}}$ as the electric voltages and the electric-field intensity on the external and internal surface, respectively, then the following relations are obtained:

$$E^{(i)}_{\mathrm{T}} = V^{(i)}_{\mathrm{T}}/h^{\mathrm{p}}, E^{(i)}_{\mathrm{B}} = V^{(i)}_{\mathrm{B}}/h^{\mathrm{p}} \tag{9}$$

According to Eqs. (2) and (6), the membrane stress resultants $N^{(i)\mathrm{p}}$ and stress couples $M^{(i)\mathrm{p}}$ of piezoelectric layers can be written as

$$\begin{bmatrix}[N^{(i)\mathrm{p}}]\\ [M^{(i)\mathrm{p}}]\end{bmatrix} = \begin{bmatrix}[A^{(i)\mathrm{p}}] & [B^{(i)\mathrm{p}}]\\ [B^{(i)\mathrm{p}}] & [D^{(i)\mathrm{p}}]\end{bmatrix}\begin{Bmatrix}[\varepsilon^{(i)}]\\ [\kappa^{(i)}]\end{Bmatrix} - \begin{bmatrix}[N^{(i)\mathrm{p}}_{\mathrm{E}}]\\ [M^{(i)\mathrm{p}}_{\mathrm{E}}]\end{bmatrix} = \begin{bmatrix}[A^{(i)\mathrm{p}}_{jl}] & [B^{(i)\mathrm{p}}_{jl}]\\ [B^{(i)\mathrm{p}}_{jl}] & [D^{(i)\mathrm{p}}_{jl}]\end{bmatrix}\begin{Bmatrix}[\varepsilon^{(i)}]\\ [\kappa^{(i)}]\end{Bmatrix} - \begin{bmatrix}\int_{\Omega^{(i)\mathrm{p}}}[e]^{\mathrm{T}}[E^{(i)}]\mathrm{d}z\\ \int_{\Omega^{(i)\mathrm{p}}}[e]^{\mathrm{T}}[E^{(i)}]z\mathrm{d}z\end{bmatrix} \tag{10}$$

where the last item is the change of stress resultants and stress couples after voltages are applied on piezoelectric layer, and

$$[N^{(i)\mathrm{p}}]=\begin{Bmatrix} N_x^{(i)\mathrm{p}} \\ N_y^{(i)\mathrm{p}} \\ N_{xy}^{(i)\mathrm{p}} \end{Bmatrix},\quad [M^{(i)\mathrm{p}}]=\begin{Bmatrix} M_x^{(i)\mathrm{p}} \\ M_y^{(i)\mathrm{p}} \\ M_{xy}^{(i)\mathrm{p}} \end{Bmatrix},\quad [N_{\mathrm{E}}^{(i)\mathrm{p}}]=\begin{Bmatrix} N_{\mathrm{E}x}^{(i)\mathrm{p}} \\ N_{\mathrm{E}y}^{(i)\mathrm{p}} \\ N_{\mathrm{E}xy}^{(i)\mathrm{p}} \end{Bmatrix},\quad [M_{\mathrm{E}}^{(i)\mathrm{p}}]=\begin{Bmatrix} M_{\mathrm{E}x}^{(i)\mathrm{p}} \\ M_{\mathrm{E}y}^{(i)\mathrm{p}} \\ M_{\mathrm{E}xy}^{(i)\mathrm{p}} \end{Bmatrix} \tag{11}$$

$$(A_{jl}^{(i)\mathrm{p}}, B_{jl}^{(i)\mathrm{p}}, D_{jl}^{(i)\mathrm{p}}) = \int_{\Omega_{\mathrm{ip}}} Q_{jl}^{p}(1,z,z^2)\mathrm{d}z(j,l=1,2,6)$$

where $A_{jl}^{(i)\mathrm{p}}, B_{jl}^{(i)\mathrm{p}}, D_{jl}^{(i)\mathrm{p}}$ are the extension, coupling and bending rigidity of region $\Omega^{(i)\mathrm{p}}$ respectively.

From Eqs. (4) and (10), the membrane stress resultants $N^{(i)}$ and stress couples $M^{(i)}$ of piezoelectric laminated cylindrical shell can be written as

$$\begin{aligned}\begin{Bmatrix} [N^{(i)}] \\ [M^{(i)}] \end{Bmatrix} &= \begin{Bmatrix} [N^{(i)\mathrm{e}}] \\ [M^{(i)\mathrm{e}}] \end{Bmatrix} + \begin{Bmatrix} [N^{(i)\mathrm{p}}] \\ [M^{(i)\mathrm{p}}] \end{Bmatrix} = \begin{bmatrix} [A^{(i)}] & [B^{(i)}] \\ [B^{(i)}] & [D^{(i)}] \end{bmatrix}\begin{Bmatrix} [\varepsilon^{(i)}] \\ [\kappa^{(i)}] \end{Bmatrix} - \begin{Bmatrix} [N_{\mathrm{E}}^{(i)\mathrm{p}}] \\ [M_{\mathrm{E}}^{(i)\mathrm{p}}] \end{Bmatrix} \\ &= \begin{bmatrix} [A^{(i)\mathrm{e}}+A^{(i)\mathrm{p}}] & [B^{(i)\mathrm{e}}+B^{(i)\mathrm{p}}] \\ [B^{(i)\mathrm{e}}+B^{(i)\mathrm{p}}] & [D^{(i)\mathrm{e}}+D^{(i)\mathrm{p}}] \end{bmatrix}\begin{Bmatrix} [\varepsilon^{(i)}] \\ [\kappa^{(i)}] \end{Bmatrix} - \begin{Bmatrix} [N_{\mathrm{E}}^{(i)\mathrm{p}}] \\ [M_{\mathrm{E}}^{(i)\mathrm{p}}] \end{Bmatrix}\end{aligned} \tag{12}$$

2.2. Analysis of contact force

The contact will emerge in the delamination regions when the piezoelectric laminated cylindrical shell is subjected to transverse periodic load, thereby the contact effect should be taken into account. Supposing q^* is the contact force per unit length perpendicular to x-axis and it acts on the delamination surface, the contact force q^* should satisfy the following condition:

$$q^* = \begin{cases} 0 & \text{if } w^{(2)} - w^{(3)} \leqslant 0 \\ f(w^{(2)} - w^{(3)}) & \text{if } w^{(2)} - w^{(3)} > 0 \end{cases} \tag{13}$$

According to Hertz contact law, the function $f(w^{(2)} - w^{(3)})$ can be chosen as a nonlinear spring function (Chen and Wang, 2006; Schwarts, 2007a,b; Wang, 2002), that is

$$f(w^{(2)} - w^{(3)}) = k_{\mathrm{h}}(w^{(2)} - w^{(3)})^{3/2} \tag{14}$$

where k_{h} is the stiffness factor of contact region and need to be derived by experiment.

It is noted that for any $w^{(2)} - w^{(3)}$, q^* in Eq. (13) can be expressed as

$$q^* = \max[f_1(w^{(2)} - w^{(3)}), f_2(w^{(2)} - w^{(3)})] \tag{15}$$

where

$$\begin{aligned} &f_1(w^{(2)} - w^{(3)}) = 0 \\ &f_2(w^{(2)} - w^{(3)}) = k_{\mathrm{h}}[\mathrm{sign}(w^{(2)} - w^{(3)})](|w^{(2)} - w^{(3)}|)^{3/2} \\ &\mathrm{sign}(x) = \begin{cases} 1 & x \geqslant 0 \\ -1 & x < 0 \end{cases} \end{aligned} \tag{16}$$

The q^* in Eq. (13) can be approximated by the following expression:

$$q^* = \alpha(f_1, f_2)f_1 + \beta(f_1, f_2)f_2 \tag{17}$$

where $\alpha(f_1, f_2)$ and $\beta(f_1, f_2)$ are functions of f_1 and f_2, and they should satisfy the following conditions:

$$\begin{aligned} &\text{if } f_1 > f_2, \alpha \to 1, \beta \to 0 \\ &\text{if } f_1 \leqslant f_2, \alpha \to 0, \beta \to 1 \end{aligned} \tag{18}$$

$\alpha(f_1, f_2)$ and $\beta(f_1, f_2)$ can be chosen as

$$\begin{aligned} \alpha(f_1, f_2) &= \frac{1}{2}[1 + \tanh A(f_1 - f_2)] \\ \beta(f_1, f_2) &= \frac{1}{2}[1 - \tanh A(f_1 - f_2)] \end{aligned} \tag{19}$$

where the parameters A is an artificially chosen large number depending upon the desired accuracy of approximation. (The A is taken as 10^{15} in present study.)

From Eqs. (16), (17) and (19), the contact force q^* can be approximated by

$$q^* = \frac{1}{2}[1+\tanh(Af_2)]f_2 \tag{20}$$

Substituting f_2 in Eq. (16) into the above equation, then we have

$$q^* = \frac{1}{2}[1+\tanh(Ak_h(\mathrm{sign}(w^{(2)}-w^{(3)}))(|w^{(2)}-w^{(3)}|)^{3/2})]k_h(\mathrm{sign}(w^{(2)}-w^{(3)}))(|w^{(2)}-w^{(3)}|)^{3/2} \tag{21}$$

Eq. (21) is the formula of nonlinear calculating contact force between delamination regions.

2.3. Analysis of energy

The total potential energy of the delaminated piezoelectric laminated cylindrical shell can be written as

$$\begin{aligned}\mathbf{\Pi} = &\sum_{i=1}^{4}\int\int\int_{\Omega^{(i)\mathrm{e}}} U^{(i)\mathrm{e}}\mathrm{d}x\mathrm{d}y\mathrm{d}z - \frac{1}{2}\sum_{i=1}^{4}\int\int_{A_i}(\rho^{\mathrm{e}}h^{(i)\mathrm{e}}+\rho^{\mathrm{p}}h^{(i)\mathrm{p}})\{d\}_{,t}^{(i)}\{d\}_{,t}^{(i)\mathrm{T}}\mathrm{d}x\mathrm{d}y - \sum_{i=1}^{4}\int\int_{A_i} q^{(i)}w^{(i)}\mathrm{d}x\mathrm{d}y \\ &-\sum_{i=1}^{4}\int\int_{A_i} T_{\mathrm{c}}^{(i)}\frac{q^*}{2\pi R_{\mathrm{d}}}w^{(i)}\mathrm{d}x\mathrm{d}y + \sum_{i=1}^{4}\int\int\int_{\Omega^{(i)\mathrm{p}}} H^{(i)\mathrm{p}}\mathrm{d}x\mathrm{d}y\mathrm{d}z\end{aligned} \tag{22}$$

where $U^{(i)\mathrm{e}}$ is the strain energy density relative to region $\Omega^{(i)\mathrm{e}}$. $\{d\}^{(i)}$ is the displacement vector, that is, $\{d\}^{(i)} = \{u^{(i)}, v^{(i)}, w^{(i)}\}$. $q^{(i)}$ is the external load of each region. $T_{\mathrm{c}}^{(i)}$ is the coefficient of contact effect and $T_{\mathrm{c}}^{(1)} = T_{\mathrm{c}}^{(4)} = 0, T_{\mathrm{c}}^{(2)} = -1$, $T_{\mathrm{c}}^{(3)} = 1$, R_{d} is the curvature radius of delamination interface. $H^{(i)\mathrm{p}}$ is the enthalpy density (Shi, 2003; Xu, 2000; Chen, 2003) relative to region $\Omega^{(i)\mathrm{p}}$ of piezoelectric layer, $h^{(i)\ \mathrm{p}}$ is the thickness of region $\Omega^{(i)\ \mathrm{p}}$, and applying Eq. (7), we have

$$\begin{aligned}&\textstyle\sum_{i=1}^{4}\int\int\int_{\Omega^{(i)\mathrm{p}}} H^{(i)\mathrm{p}}\mathrm{d}x\mathrm{d}y\mathrm{d}z = \sum_{i=1}^{4}\int\int\int_{\Omega^{(i)\mathrm{p}}}\left\{U^{(i)\mathrm{p}} - [E^{(i)}]^{\mathrm{T}}[e]([\varepsilon^{(i)}]+z[\kappa^{(i)}]) - \frac{1}{2}[E^{(i)}]^{\mathrm{T}}[\varepsilon^*][E^{(i)}]\right\}\mathrm{d}x\mathrm{d}y\mathrm{d}z \\ &= \sum_{i=1}^{4}\int\int_{A_i}\left\{\frac{1}{2}\begin{Bmatrix}[\varepsilon^{(i)}+\delta\varepsilon^{(i)}]\\ [\kappa^{(i)}+\delta\kappa^{(i)}]\end{Bmatrix}^{\mathrm{T}}\begin{bmatrix}[A^{(i)\mathrm{p}}] & [B^{(i)\mathrm{p}}]\\ [B^{(i)\mathrm{p}}] & [D^{(i)\mathrm{p}}]\end{bmatrix}\begin{Bmatrix}[\varepsilon^{(i)}+\delta\varepsilon^{(i)}]\\ [\kappa^{(i)}+\delta\kappa^{(i)}]\end{Bmatrix} - \begin{Bmatrix}[N_{\mathrm{E}}^{(i)\mathrm{p}}]\\ [M_{\mathrm{E}}^{(i)\mathrm{p}}]\end{Bmatrix}^{\mathrm{T}}\begin{Bmatrix}[\varepsilon^{(i)}]\\ [\kappa^{(i)}]\end{Bmatrix}\right. \\ &\quad\left. - \frac{1}{2}\int_{\Omega^{(i)\mathrm{p}}}\{[E^{(i)}]^{\mathrm{T}}[\varepsilon^*][E^{(i)}]\}\mathrm{d}z\right\}\mathrm{d}x\mathrm{d}y\end{aligned} \tag{23}$$

where $U^{(i)\mathrm{p}}$ is the strain energy density relative to region $\Omega^{(i)\mathrm{p}}$, and we define

$$\frac{1}{2}\int_{\Omega_i}\{[E^{(i)}]^{\mathrm{T}}[\varepsilon^*][E^{(i)}]\}\mathrm{d}z = \frac{1}{2}\int_{\Omega_i}\varepsilon_{33}^*E_z^{(i)2}\mathrm{d}z = \frac{1}{2}\varepsilon_{33}^*\int_{\Omega_i}E_z^{(i)2}\mathrm{d}z \triangleq = C_{\mathrm{E}}^{(i)} \tag{24}$$

Using Eqs. (23) and (24) and noticing that the problem of delamination growth is the variation of moving boundary, then from Eq. (22), the variation of the total potential energy of delaminated piezoelectric laminated cylindrical shell is

$$\begin{aligned}\delta\mathbf{\Pi} = &\sum_{i=1}^{4}\int\int_{A_i+\delta A_i}\frac{1}{2}\begin{Bmatrix}[\varepsilon^{(i)}+\delta\varepsilon^{(i)}]\\ [\kappa^{(i)}+\delta\kappa^{(i)}]\end{Bmatrix}^{\mathrm{T}}\begin{bmatrix}[A^{(i)}] & [B^{(i)}]\\ [B^{(i)}] & [D^{(i)}]\end{bmatrix}\begin{Bmatrix}[\varepsilon^{(i)}+\delta\varepsilon^{(i)}]\\ [\kappa^{(i)}+\delta\kappa^{(i)}]\end{Bmatrix}\mathrm{d}x\mathrm{d}y \\ &-\frac{1}{2}\sum_{i=1}^{4}\int\int_{A_i+\delta A_i}(\rho^{\mathrm{e}}h^{(i)\mathrm{e}}+\rho^{\mathrm{p}}h^{(i)\mathrm{p}})(\{d\}_{,t}^{(i)}+\delta\{d\}_{,t}^{(i)})(\{d\}_{,t}^{(i)}+\delta\{d\}_{,t}^{(i)})^{\mathrm{T}}\mathrm{d}x\mathrm{d}y \\ &-\sum_{i=1}^{4}\int\int_{A_i+\delta A_i}q^{(i)}(w^{(i)}+\delta w^{(i)})\mathrm{d}x\mathrm{d}y - \sum_{i=1}^{4}\int\int_{A_i+\delta A_i}\left\{\begin{Bmatrix}[N_{\mathrm{E}}^{(i)\mathrm{p}}]\\ [M_{\mathrm{E}}^{(i)\mathrm{p}}]\end{Bmatrix}^{\mathrm{T}}\begin{Bmatrix}[\varepsilon^{(i)}+\delta\varepsilon^{(i)}]\\ [\kappa^{(i)}+\delta\kappa^{(i)}]\end{Bmatrix}+C_{\mathrm{E}}^{(i)}\right\}\mathrm{d}x\mathrm{d}y \\ &-\sum_{i=1}^{4}\int\int_{A_i+\delta A_i}T_{\mathrm{c}}^{(i)}\frac{q^*}{2\pi R_{\mathrm{d}}}(w^{(i)}+\delta w^{(i)})\mathrm{d}x\mathrm{d}y - \mathbf{\Pi}\end{aligned} \tag{25}$$

where the first item of Eq. (25) is the strain energy in region $\Omega^{(i)}$ of piezoelectric laminated cylindrical shell after the growth of delamination. Assuming the laminated cylindrical shells are symmetrically laminated, then $[B^{(i)}] = 0$. After calculating the integration by parts to time variable, the Eq. (25) can be written as

$$\begin{aligned}\delta\mathbf{\Pi} = &\sum_{i=1}^{4}\int\int_{A_i}\{[\varepsilon^{(i)}]^{\mathrm{T}}[A^{(i)}][\delta\varepsilon^{(i)}]+[\kappa^{(i)}]^{\mathrm{T}}[D^{(i)}][\delta\kappa^{(i)}]\}\mathrm{d}x\mathrm{d}y + \sum_{i=1}^{4}\int\int_{A_i}(\rho^{\mathrm{e}}h^{(i)\mathrm{e}}+\rho^{\mathrm{p}}h^{(i)\mathrm{p}})\{d\}_{,tt}^{(i)}\delta\{d\}^{(i)\mathrm{T}}\mathrm{d}x\mathrm{d}y \\ &-\sum_{i=1}^{4}\int\int_{A_i}q^{(i)}\delta w^{(i)}\mathrm{d}x\mathrm{d}y - \sum_{i=1}^{4}\int\int_{A_i}T_{\mathrm{c}}^{i}\frac{q^*}{2\pi R_{\mathrm{d}}}\delta w^{(i)}\mathrm{d}x\mathrm{d}y - \sum_{i=1}^{4}\int\int_{A_i}\begin{Bmatrix}[N_{\mathrm{E}}^{(i)\mathrm{p}}]\\ [M_{\mathrm{E}}^{(i)\mathrm{p}}]\end{Bmatrix}^{\mathrm{T}}\begin{Bmatrix}[\delta\varepsilon^{(i)}]\\ [\delta\kappa^{(i)}]\end{Bmatrix}\mathrm{d}x\mathrm{d}y \\ &+\frac{1}{2}\sum_{i=1}^{4}\int\int_{\delta A_i}\{[\varepsilon^{(i)}]^{\mathrm{T}}[A^{(i)}][\varepsilon^{(i)}]+[\kappa^{(i)}]^{\mathrm{T}}[D^{(i)}][\kappa^{(i)}]\}\mathrm{d}x\mathrm{d}y + \frac{1}{2}\sum_{i=1}^{4}\int\int_{\delta A_i}(\rho^{\mathrm{e}}h^{(i)\mathrm{e}}+\rho^{\mathrm{p}}h^{(i)\mathrm{p}})\{d\}_{,tt}^{(i)}\{d\}^{(i)\mathrm{T}}\mathrm{d}x\mathrm{d}y \\ &-\sum_{i=1}^{4}\int\int_{\delta A_i}q^{(i)}w^{(i)}\mathrm{d}x\mathrm{d}y - \sum_{i=1}^{4}\int\int_{\delta A_i}T_{\mathrm{c}}^{(i)}\frac{q^*}{2\pi R_{\mathrm{d}}}w^{(i)}\mathrm{d}x\mathrm{d}y - \sum_{i=1}^{4}\int\int_{\delta A_i}\{[N_{\mathrm{E}}^{(i)\mathrm{p}}]^{\mathrm{T}}[\varepsilon^{(i)}]+[M_{\mathrm{E}}^{(i)\mathrm{p}}]^{\mathrm{T}}[\kappa^{(i)}]+C_{\mathrm{E}}^{(i)}\}\mathrm{d}x\mathrm{d}y\end{aligned} \tag{26}$$

The last five items of Eq. (26) can be written as

$$\begin{aligned}&\tfrac{1}{2}\sum_{i=1}^{4}\int\int_{\delta A_i}\{[\varepsilon^{(i)}]^{\mathrm{T}}[A^{(i)}][\varepsilon^{(i)}]+[\kappa^{(i)}]^{\mathrm{T}}[D^{(i)}][\kappa^{(i)}]\}\mathrm{d}x\mathrm{d}y+\tfrac{1}{2}\sum_{i=1}^{4}\int\int_{\delta A_i}(\rho^{\mathrm{e}}h^{(i)\mathrm{e}}+\rho^{\mathrm{p}}h^{(i)\mathrm{p}})\{d\}^{(i)}_{,tt}\{d\}^{(i)\mathrm{T}}\mathrm{d}x\mathrm{d}y\\&-\sum_{i=1}^{4}\int\int_{\delta A_i}q^{(i)}w^{(i)}\mathrm{d}x\mathrm{d}y-\sum_{i=1}^{4}\int\int_{\delta A_i}T^{(i)}_{\mathrm{c}}\tfrac{q^*}{2\pi R_{\mathrm{d}}}w^{(i)}\mathrm{d}x\mathrm{d}y-\sum_{i=1}^{4}\int\int_{\delta A_i}\{[N^{(i)\mathrm{p}}_{\mathrm{E}}]^{\mathrm{T}}[\varepsilon^{(i)}]+[M^{(i)\mathrm{p}}_{\mathrm{E}}]^{\mathrm{T}}[\kappa^{(i)}]+C^{(i)}_{\mathrm{E}}\}\mathrm{d}x\mathrm{d}y\\&=\sum_{i=1}^{4}\int_{C_j}\{\tfrac{1}{2}([\varepsilon^{(i)}]^{\mathrm{T}}[A^{(i)}][\varepsilon^{(i)}]+[\kappa^{(i)}]^{\mathrm{T}}[D^{(i)}][\kappa^{(i)}])+\tfrac{1}{2}(\rho^{\mathrm{e}}h^{(i)\mathrm{e}}+\rho^{\mathrm{p}}h^{(i)\mathrm{p}})\{d\}^{(i)}_{,tt}\{d\}^{(i)\mathrm{T}}-q^{(i)}w^{(i)}\\&-T^{(i)}_{\mathrm{c}}\tfrac{q^*}{2\pi R_{\mathrm{d}}}w^{(i)}-([N^{(i)\mathrm{p}}_{\mathrm{E}}]^{\mathrm{T}}[\varepsilon^{(i)}]+[M^{(i)\mathrm{p}}_{\mathrm{E}}]^{\mathrm{T}}[\kappa^{(i)}]+C^{(i)}_{\mathrm{E}})\}\delta n_i\mathrm{d}C_j(j=1,2)\end{aligned}\tag{27}$$

As the variation of $u^{(i)}$, $v^{(i)}$, $w^{(i)}$ is carried out on variable boundary C_j, the following conditions should be satisfied:

$$\begin{aligned}&\delta u^{(i)}|_{C_j}=\delta(u^{(i)}|_{C_j})-\frac{\partial u^{(i)}}{\partial n}\bigg|_{C_j}\cdot\delta n_i,\delta v^{(i)}|_{C_j}=\delta(v^{(i)}|_{C_j})-\frac{\partial v^{(i)}}{\partial n}\bigg|_{C_j}\cdot\delta n_i,\delta w^{(i)}|_{C_j}=\delta(w^{(i)}|_{C_j})-\frac{\partial w^{(i)}}{\partial n}\bigg|_{C_j}\cdot\delta n_i\\&\delta w^{(i)}_{,x}|_{C_j}=\delta(w^{(i)}_{,x}|_{C_j})-\frac{\partial w^{(i)}_{,x}}{\partial n}\bigg|_{C_j}\cdot\delta n_i,\delta w^{(i)}_{,y}|_{C_j}=\delta(w^{(i)}_{,y}|_{C_j})-\frac{\partial w^{(i)}_{,y}}{\partial n}\bigg|_{C_j}\cdot\delta n_i\end{aligned}\tag{28}$$

Using Eqs. (4)–(12) and Eqs. (27) and (28), according to Eq. (26), we have

$$\begin{aligned}\delta\boldsymbol{\Pi}=&\sum_{i=1}^{4}\int\int_{A_i}\left\{\left[-\frac{\partial}{\partial x}(N^{(i)}_x)-\frac{\partial}{\partial y}(N^{(i)}_{xy})+(\rho^{\mathrm{e}}h^{(i)\mathrm{e}}+\rho^{\mathrm{p}}h^{(i)\mathrm{p}})u^{(i)}_{,tt}\right]\delta u^{(i)}+\left[-\frac{\partial}{\partial x}(N^{(i)}_{xy})\right.\right.\\&\left.-\frac{\partial}{\partial y}(N^{(i)}_y)+(\rho^{\mathrm{e}}h^{(i)\mathrm{e}}+\rho^{\mathrm{p}}h^{(i)\mathrm{p}})v^{(i)}_{,tt}\right]\delta v^{(i)}+\left[-\frac{\partial}{\partial x}(M^{(i)}_{x,x})-\frac{\partial}{\partial y}(M^{(i)}_{y,y})-\frac{\partial}{\partial y}(M^{(i)}_{xy,x})\right.\\&-\frac{\partial}{\partial x}(M^{(i)}_{xy,y})-\frac{\partial}{\partial x}(N^{(i)}_xw^{(i)}_{,x})-\frac{\partial}{\partial y}(N^{(i)}_yw^{(i)}_{,y})-\frac{\partial}{\partial x}(N^{(i)}_{xy}w^{(i)}_{,y})-\frac{\partial}{\partial y}(N^{(i)}_{xy}w^{(i)}_{,x})-\frac{N^{(i)}_y}{R^{(i)}}\\&\left.\left.+(\rho^{\mathrm{e}}h^{(i)\mathrm{e}}+\rho^{\mathrm{p}}h^{(i)\mathrm{p}})w^{(i)}_{,tt}-q^{(i)}-T^{(i)}_{\mathrm{c}}\frac{q^*}{2\pi R_{\mathrm{d}}}\right]\delta w^{(i)}\right\}\mathrm{d}x\mathrm{d}y+\sum_{i=1}^{4}\int_{C_j}\{N^{(i)}_x\delta(u^{(i)}|_{C_j})\\&+N^{(i)}_{xy}\delta(v^{(i)}|_{C_j})+(M^{(i)}_{x,x}+M^{(i)}_{xy,y}+N^{(i)}_xw^{(i)}_{,x}+N^{(i)}_{xy}w^{(i)}_{,y})\delta(w^{(i)}|_{C_j})-M^{(i)}_x\delta(w^{(i)}_{,x}|_{C_j})\\&-M^{(i)}_{xy}\delta(w^{(i)}_{,y}|_{C_j})\}\mathrm{d}C_j+\sum_{i=1}^{4}\oint_{C_j}[N^{(i)}_x\left(-\frac{\partial u^{(i)}}{\partial n}\bigg|_{C_j}\right)+N^{(i)}_{xy}\left(-\frac{\partial v^{(i)}}{\partial n}\bigg|_{C_j}\right)+(M^{(i)}_{x,x}\\&\left.+M^{(i)}_{xy,y}+N^{(i)}_xw^{(i)}_{,x}+N^{(i)}_{xy}w^{(i)}_{,y})\left(-\frac{\partial w^{(i)}}{\partial n}\bigg|_{C_j}\right)+M^{(i)}_x\frac{\partial w^{(i)}_{,x}}{\partial n}\bigg|_{C_j}+M^{(i)}_{xy}\frac{\partial w^{(i)}_{,y}}{\partial n}\bigg|_{C_j}\right]\cdot\delta n_i\mathrm{d}C_j\\&+\sum_{i=1}^{4}\int_{C_j}\left\{\frac{1}{2}[N^{(i)}_x(u^{(i)}_{,x}+\frac{1}{2}w^{(i)2}_{,x})+N^{(i)}_y(v^{(i)}_{,y}-\frac{w^{(i)}}{R^{(i)}}+\frac{1}{2}w^{(i)2}_{,y})+N^{(i)}_{xy}(u^{(i)}_{,y}+v^{(i)}_{,x}+w^{(i)}_{,x}w^{(i)}_{,y})\right.\\&+M^{(i)}_x(-w^{(i)}_{,xx})+M^{(i)}_y(-w^{(i)}_{,yy})+M^{(i)}_{xy}(-2w^{(i)}_{,xy})]+\frac{1}{2}(\rho^{\mathrm{e}}h^{(i)\mathrm{e}}+\rho^{\mathrm{p}}h^{(i)\mathrm{p}})\{d\}^{(i)}_{,tt}\{d\}^{(i)\mathrm{T}}\\&\left.-q^{(i)}w^{(i)}-T^{(i)}_{\mathrm{c}}\frac{q^*}{2\pi R_{\mathrm{d}}}w^{(i)}-\frac{1}{2}([N^{(i)\mathrm{p}}_{\mathrm{E}}]^{\mathrm{T}}[\varepsilon^{(i)}]+[M^{(i)\mathrm{p}}_{\mathrm{E}}]^{\mathrm{T}}[\kappa^{(i)}]+2C^{(i)}_{\mathrm{E}})\right\}\delta n_i\mathrm{d}C_j\end{aligned}\tag{29}$$

The Eq. (29) is written as the following two parts, that is

$$\delta\boldsymbol{\Pi}=\delta\boldsymbol{\Pi}_1+\delta\boldsymbol{\Pi}_2\tag{30}$$

where

$$\begin{aligned}\delta\boldsymbol{\Pi}_1=&\sum_{i=1}^{4}\int\int_{A_i}\left\{\left[-\frac{\partial}{\partial x}(N^{(i)}_x)-\frac{\partial}{\partial y}(N^{(i)}_{xy})+(\rho^{\mathrm{e}}h^{(i)\mathrm{e}}+\rho^{\mathrm{p}}h^{(i)\mathrm{p}})u^{(i)}_{,tt}\right]\delta u_i+\left[-\frac{\partial}{\partial x}(N^{(i)}_{xy})\right.\right.\\&\left.-\frac{\partial}{\partial y}(N^{(i)}_y)+(\rho^{\mathrm{e}}h^{(i)\mathrm{e}}+\rho^{\mathrm{p}}h^{(i)\mathrm{p}})v^{(i)}_{,tt}\right]\delta v^{(i)}+\left[-\frac{\partial}{\partial x}(M^{(i)}_{x,x})-\frac{\partial}{\partial y}(M^{(i)}_{y,y})-\frac{\partial}{\partial y}(M^{(i)}_{xy,x})\right.\\&-\frac{\partial}{\partial x}(M^{(i)}_{xy,y})-\frac{\partial}{\partial x}(N^{(i)}_xw^{(i)}_{,x})-\frac{\partial}{\partial y}(N^{(i)}_yw^{(i)}_{,y})-\frac{\partial}{\partial x}(N^{(i)}_{xy}w^{(i)}_{,y})-\frac{\partial}{\partial y}(N^{(i)}_{xy}w^{(i)}_{,x})-\frac{N^{(i)}_y}{R^{(i)}}\\&\left.\left.+(\rho^{\mathrm{e}}h^{(i)\mathrm{e}}+\rho^{\mathrm{p}}h^{(i)\mathrm{p}})w^{(i)}_{,tt}-q^{(i)}-T^{(i)}_{\mathrm{c}}\frac{q^*}{2\pi R_{\mathrm{d}}}\right]\delta w^{(i)}\right\}\mathrm{d}x\mathrm{d}y+\sum_{i=1}^{4}\int_{C_j}\{N^{(i)}_x\delta(u^{(i)}|_{C_j})\\&+N^{(i)}_{xy}\delta(v^{(i)}|_{C_j})+(M^{(i)}_{x,x}+M^{(i)}_{xy,y}+N^{(i)}_xw^{(i)}_{,x}+N^{(i)}_{xy}w^{(i)}_{,y})\delta(w^{(i)}|_{C_j})-M^{(i)}_x\delta(w^{(i)}_{,x}|_{C_j})\\&-M^{(i)}_{xy}\delta(w^{(i)}_{,y}|_{C_j})\Big\}\mathrm{d}C_j\end{aligned}\tag{31}$$

$$\begin{aligned}\delta\mathbf{\Pi}_2 = &\sum_{i=1}^{4}\oint_{C_j}\{[N_x^{(i)}\left(-\frac{\partial u^{(i)}}{\partial n}\bigg|_{C_j}\right)+N_{xy}^{(i)}\left(-\frac{\partial v^{(i)}}{\partial n}\bigg|_{C_j}\right)+(M_{x,x}^{(i)}+M_{xy,y}^{(i)}+N_x^{(i)}w_{,x}^{(i)}+N_{xy}^{(i)}w_{,y}^{(i)})\\ &\times\left(-\frac{\partial w^{(i)}}{\partial n}\bigg|_{C_j}\right)+M_x^{(i)}\frac{\partial w_{,x}^{(i)}}{\partial n}\bigg|_{C_j}+M_{xy}^{(i)}\frac{\partial w_{,y}^{(i)}}{\partial n}\bigg|_{C_j}]\cdot\delta n_i\mathrm{d}C_j+\sum_{i=1}^{4}\int_{C_j}\{\frac{1}{2}[N_x^{(i)}(u_{,x}^{(i)}+\frac{1}{2}w_{,x}^{(i)2})\\ &+N_y^{(i)}(v_{,y}^{(i)}-\frac{w^{(i)}}{R^{(i)}}+\frac{1}{2}w_{,y}^{(i)2})+N_{xy}^{(i)}(u_{,y}^{(i)}+v_{,x}^{(i)}+w_{,x}^{(i)}w_{,y}^{(i)})+M_x^{(i)}(-w_{,xx}^{(i)})+M_y^{(i)}(-w_{,yy}^{(i)})\\ &+M_{xy}^{(i)}(-2w_{,xy}^{(i)})]+\frac{1}{2}(\rho^{\mathrm{e}}h^{(i)\mathrm{e}}+\rho^{\mathrm{p}}h^{(i)\mathrm{p}})\{d\}_{,tt}^{(i)}\{d\}^{(i)\mathrm{T}}-q^{(i)}w^{(i)}-T_{\mathrm{c}}^{(i)}\frac{q^*}{2\pi R_{\mathrm{d}}}w^{(i)}\\ &-\frac{1}{2}([N_{\mathrm{E}}^{(i)\mathrm{p}}]^{\mathrm{T}}[\varepsilon^{(i)}]+[M_{\mathrm{E}}^{(i)\mathrm{p}}]^{\mathrm{T}}[\kappa^{(i)}]+2C_{\mathrm{E}}^{(i)}]\}\delta n_i\mathrm{d}C_j\end{aligned} \tag{32}$$

Here, $\delta\mathbf{\Pi}_1$ is the variation of potential energy due to the virtual displacement of piezoelectric laminated cylindrical shell while virtual growth does not occur (i.e. the delamination boundary is immovable). According to the principle of virtual displacement, when the shell is in state of equilibrium, we have

$$\delta\mathbf{\Pi}_1 = 0 \tag{33}$$

The displacement of laminated cylindrical shell must change after virtual growth δn occurs along delamination front. At the same time, the changed area in the region of integration is that $\delta A_i = \int_{C_j}\delta n_i \mathrm{d}C_j$. Thus, $\delta\mathbf{\Pi}_2$ is the variation of potential energy due to the area variation of each region.

As for piezoelectric laminated cylindrical shell, the normal direction n of delamination growth boundary is consistent with the axial direction x. Therefore, Eq. (32) can also be written as follows:

$$\begin{aligned}\delta\mathbf{\Pi}_2 = &\sum_{i=1}^{4}\oint_{C_j}[N_x^{(i)}(-u_{,x}^{(i)})+N_{xy}^{(i)}(-v_{,x}^{(i)})+(M_{x,x}^{(i)}+M_{xy,y}^{(i)}+N_x^{(i)}w_{,x}^{(i)}+N_{xy}^{(i)}w_{,y}^{(i)})(-w_{,x}^{(i)})\\ &+M_x^{(i)}w_{,xx}^{(i)}+M_{xy}^{(i)}w_{,xy}^{(i)}]\cdot\delta n_i\mathrm{d}C_j+\sum_{i=1}^{4}\oint_{C_j}\left\{\frac{1}{2}\left[N_x^{(i)}(u_{,x}^{(i)}+\frac{1}{2}w_{,x}^{(i)2})+N_y^{(i)}(v_{,y}^{(i)}-\frac{w^{(i)}}{R^{(i)}}\right.\right.\\ &\left.+\frac{1}{2}w_{,y}^{(i)2})+N_{xy}^{(i)}(u_{,y}^{(i)}+v_{,x}^{(i)}+w_{,x}^{(i)}w_{,y}^{(i)})+M_x^{(i)}(-w_{,xx}^{(i)})+M_y^{(i)}(-w_{,yy}^{(i)})+M_{xy}^{(i)}(-2w_{,xy}^{(i)})\right]\\ &+\frac{1}{2}(\rho^{\mathrm{e}}h^{(i)\mathrm{e}}+\rho^{\mathrm{p}}h^{(i)\mathrm{p}})\{d\}_{,tt}^{(i)}\{d\}^{(i)\mathrm{T}}-q^{(i)}w^{(i)}-T_{\mathrm{c}}^{(i)}(q^*/2\pi R_{\mathrm{d}})w^{(i)}-\frac{1}{2}\left[N_{\mathrm{E}x}^{(i)\mathrm{p}}(u_{,x}^{(i)}\right.\\ &+\frac{1}{2}w_{,x}^{(i)2})+N_{\mathrm{E}y}^{(i)\mathrm{p}}\left(v_{,y}^{(i)}-\frac{w^{(i)}}{R^{(i)}}+\frac{1}{2}w_{,y}^{(i)2}\right)+N_{\mathrm{E}xy}^{(i)\mathrm{p}}(u_{,y}^{(i)}+v_{,x}^{(i)}+w_{,x}^{(i)}w_{,y}^{(i)})+M_{\mathrm{E}x}^{(i)\mathrm{p}}(-w_{,xx}^{(i)})\\ &\left.\left.+M_{\mathrm{E}y}^{(i)\mathrm{p}}(-w_{,yy}^{(i)})+M_{\mathrm{E}xy}^{(i)\mathrm{p}}(-2w_{,xy}^{(i)})+2C_{\mathrm{E}}^{(i)}\right]\right\}\delta n_i\mathrm{d}C_j\end{aligned} \tag{34}$$

2.4. Analysis of energy release rate along delamination front

From Eq. (30) and (33), (34), the variation of potential energy of piezoelectric laminated cylindrical shell can be given as

$$\begin{aligned}\delta\mathbf{\Pi} = \delta\mathbf{\Pi}_2 = &\sum_{i=1}^{4}\oint_{C_j}[N_x^{(i)}(-u_{,x}^{(i)})+N_{xy}^{(i)}(-v_{,x}^{(i)})+(M_{x,x}^{(i)}+M_{xy,y}^{(i)}+N_x^{(i)}w_{,x}^{(i)}+N_{xy}^{(i)}w_{,y}^{(i)})(-w_{,x}^{(i)})\\ &+M_x^{(i)}w_{,xx}^{(i)}+M_{xy}^{(i)}w_{,xy}^{(i)}]\cdot\delta n_i\mathrm{d}C_j+\sum_{i=1}^{4}\oint_{C_j}\left\{\frac{1}{2}\left[N_x^{(i)}(u_{,x}^{(i)}+\frac{1}{2}w_{,x}^{(i)2})+N_y^{(i)}(v_{,y}^{(i)}-\frac{w^{(i)}}{R^{(i)}}\right.\right.\\ &\left.+\frac{1}{2}w_{,y}^{(i)2})+N_{xy}^{(i)}(u_{,y}^{(i)}+v_{,x}^{(i)}+w_{,x}^{(i)}w_{,y}^{(i)})+M_x^{(i)}(-w_{,xx}^{(i)})+M_y^{(i)}(-w_{,yy}^{(i)})+M_{xy}^{(i)}(-2w_{,xy}^{(i)})\right]\\ &+\frac{1}{2}(\rho^{\mathrm{e}}h^{(i)\mathrm{e}}+\rho^{\mathrm{p}}h^{(i)\mathrm{p}})\{d\}_{,tt}^{(i)}\{d\}^{(i)\mathrm{T}}-q^{(i)}w^{(i)}-T_{\mathrm{c}}^{(i)}(q^*/2\pi R_{\mathrm{d}})w^{(i)}-\frac{1}{2}\left[N_{\mathrm{E}x}^{(i)\mathrm{p}}(u_{,x}^{(i)}\right.\\ &+\frac{1}{2}w_{,x}^{(i)2})+N_{\mathrm{E}y}^{(i)\mathrm{p}}(v_{,y}^{(i)}-\frac{w^{(i)}}{R^{(i)}}+\frac{1}{2}w_{,y}^{(i)2})+N_{\mathrm{E}xy}^{(i)\mathrm{p}}(u_{,y}^{(i)}+v_{,x}^{(i)}+w_{,x}^{(i)}w_{,y}^{(i)})+M_{\mathrm{E}x}^{(i)\mathrm{p}}(-w_{,xx}^{(i)})\\ &\left.\left.+M_{\mathrm{E}y}^{(i)\mathrm{p}}(-w_{,yy}^{(i)})+M_{\mathrm{E}xy}^{(i)\mathrm{p}}(-2w_{,xy}^{(i)})+2C_{\mathrm{E}}^{(i)}\right]\right\}\delta n_i\mathrm{d}C_j\end{aligned} \tag{35}$$

Let

$$
\begin{aligned}
G_i = & \Big[N_x^{(i)}(-u_{,x}^{(i)}) + N_{xy}^{(i)}(-v_{,x}^{(i)}) + (M_{x,x}^{(i)} + M_{xy,y}^{(i)} + N_x^{(i)}w_{,x}^{(i)} + N_{xy}^{(i)}w_{,y}^{(i)})(-w_{,x}^{(i)}) \\
& + M_x^{(i)}w_{,xx}^{(i)} + M_{xy}^{(i)}w_{,xy}^{(i)}\Big] + \frac{1}{2}\Big[N_x^{(i)}(u_{,x}^{(i)} + \frac{1}{2}w_{,x}^{(i)2}) + N_y^{(i)}(v_{,y}^{(i)} - \frac{w^{(i)}}{R^{(i)}} + \frac{1}{2}w_{,y}^{(i)2}) \\
& + N_{xy}^{(i)}(u_{,y}^{(i)} + v_{,x}^{(i)} + w_{,x}^{(i)}w_{,y}^{(i)}) + M_x^{(i)}(-w_{,xx}^{(i)}) + M_y^{(i)}(-w_{,yy}^{(i)}) + M_{xy}^{(i)}(-2w_{,xy}^{(i)})\Big] \\
& + \frac{1}{2}(\rho^{\mathrm{e}}h^{(i)\mathrm{e}} + \rho^{\mathrm{p}}h^{(i)\mathrm{p}})\{d\}_{,tt}^{(i)}\{d\}^{(i)\mathrm{T}} - q^{(i)}w^{(i)} - T_{\mathrm{c}}^{(i)}(q^*/2\pi R_{\mathrm{d}})w^{(i)} \\
& - \frac{1}{2}\Big[N_{\mathrm{E}x}^{(i)\mathrm{p}}(u_{,x}^{(i)} + \frac{1}{2}w_{,x}^{(i)2}) + N_{\mathrm{E}y}^{(i)\mathrm{p}}\left(v_{,y}^{(i)} - \frac{w^{(i)}}{R^{(i)}} + \frac{1}{2}w_{,y}^{(i)2}\right) + N_{\mathrm{E}xy}^{(i)\mathrm{p}}(u_{,y}^{(i)} + v_{,x}^{(i)} \\
& + w_{,x}^{(i)}w_{,y}^{(i)}) + M_{\mathrm{E}x}^{(i)\mathrm{p}}(-w_{,xx}^{(i)}) + M_{\mathrm{E}y}^{(i)\mathrm{p}}(-w_{,yy}^{(i)}) + M_{\mathrm{E}xy}^{(i)\mathrm{p}}(-2w_{,xy}^{(i)}) + 2C_{\mathrm{E}}^{(i)}\Big]
\end{aligned}
\tag{36}
$$

then

$$\delta\mathbf{\Pi} = \sum_{i=1}^{4}\oint_{C_j} G_i\delta n_i \mathrm{d}C_j \tag{37}$$

According to Griffith criterion, the energy release rate of piezoelectric laminated cylindrical shell along delamination front can be expressed as

$$G = -\lim_{\delta A\to 0}\frac{\delta\mathbf{\Pi}}{\delta A} \tag{38}$$

From Eqs. (37) and (38), the average energy release rate of delamination growth is

$$G_{\mathrm{a}} = -\frac{\delta\mathbf{\Pi}}{\delta A} = -\frac{\sum_{i=1}^{4}\oint_{C_j} G_i\delta n_i \mathrm{d}C_j}{\int_{C_j}\delta n \mathrm{d}C_j} \tag{39}$$

If delamination growth occurs only on partial boundary, that is, δn is greater than zero on certain boundary ΔC_j belonged to C_j and it is equal to zero on residual boundary $C_j - \Delta C_j$, then the average energy release rate of delamination growth is

$$G_a = -\frac{\sum_{i=1}^{4}\int_{\Delta C_j} G_i\delta n_i \mathrm{d}C_j}{\int_{\Delta C_j}\delta n \mathrm{d}C_j} \tag{40}$$

Obviously, the average energy release rate relates to the mode of the delamination growth, but it is generally difficult to anticipate the actual mode of delamination growth because that δn is an unknown continuous function. So it is not able to calculate directly the average energy release rate. Now, supposing ΔC_j is a small segment including a given point and letting ΔC_j infinitely finish to approach the point, then from Eq. (40) the energy release rate of any point can be given as

$$G = -\lim_{\Delta C_j\to 0}\frac{\sum_{i=1}^{4}\int_{\Delta C_j} G_i\delta n_i \mathrm{d}C_j}{\int_{\Delta C_j}\delta n \mathrm{d}C_j} \tag{41}$$

From Eq. (41), it can be seen that the G represents the distribution of energy release rate of any point on delaminated boundary.

For boundary C_1, we have

$$\delta n_1 = -\delta n_2 = -\delta n_3 = -\delta n \tag{42}$$

From Eqs. (41) and (42), the energy release rate of any point on the boundary C_1 is

$$G_{C_1} = \lim_{\Delta C_1\to 0}\frac{\int_{\Delta C_1}(G_1 - G_2 - G_3)\delta n \mathrm{d}C_1}{\int_{\Delta C_1}\delta n \mathrm{d}C_1} = G_1 - G_2 - G_3 \tag{43}$$

For boundary C_2, we have

$$\delta n_4 = -\delta n_2 = -\delta n_3 = -\delta n \tag{44}$$

From Eqs. (41) and (44), the energy release rate of any point on the boundary C_2 is

$$G_{C_2} = \lim_{\Delta C_2\to 0}\frac{\int_{\Delta C_2}(G_4 - G_2 - G_3)\delta n \mathrm{d}C_2}{\int_{\Delta C_2}\delta n \mathrm{d}C_2} = G_4 - G_2 - G_3 \tag{45}$$

According to the Paris fatigue delamination growth law (Schön, 2000; Blanco et al., 2004; Takeda, 1999), the relation between delamination growth rate and amplitude of energy release rate can be written as

$$\frac{da}{dN} = D\left(\frac{\Delta G}{G_c}\right)^r \tag{46}$$

where a is the length of delamination and $a = L^{(2)}$ in present analysis, N is cycle numbers of dynamic load, ΔG is amplitude of energy release rate, the constants D and r are determined by experiment. The experiment results of literature (Blanco et al., 2004) are applied in present analysis, that is, $D = 1.68 \times 10^{-1}$, $r = 6.28$, $G_c = 447\ \mathrm{J/m^2}$.

2.5. The nonlinear governing equations and corresponding boundary conditions and matching conditions of the axisymmetrical piezoelectric laminated cylindrical shell

As for axisymmetrical piezoelectric laminated cylindrical shell, the circumferential displacement of shell $v^{(i)} = 0$. Introducing the following dimensionless parameters:

$$\begin{aligned}
&\xi_i = \frac{x^{(i)}}{L^{(i)}}, W_i = \frac{w^{(i)}}{h^e}, U_i = \frac{u^{(i)}}{L}, Q^{(i)} = \frac{q^{(i)}L^4}{A_{22}(h^e)^3}, \alpha_i = \frac{h^{(i)}}{h^e}, \beta_i = \frac{L^{(i)}}{L}, H = \frac{L}{h^e}, \tau = \frac{t}{L^2}\sqrt{A_{22}h^e/\rho^e} \\
&N^p_{iEx} = \frac{N^{(i)p}_{Ex}}{A_{22}}, N^p_{iEy} = \frac{N^{(i)p}_{Ey}}{A_{22}}, p_i = \frac{\rho^p h^{(i)p}}{\rho^e h^e}, \bar{C}^{(i)}_E = \frac{C^{(i)}_E}{A_{22}}, K_i = \frac{L^2}{R^{(i)}h^e}, K_H = \frac{k_h(h^e)^{3/2}}{2\pi R_d}
\end{aligned} \tag{47}$$

Substituting Eqs. (31) and (47) into Eq. (33), the dimensionless nonlinear dynamic governing equations of axisymmetrical piezoelectric laminated cylindrical shell with delamination may be expressed as follows:

$$\begin{aligned}
&S_{11A}\frac{1}{\beta_i^2}U_{i,\xi\xi} - S_{12A}\frac{K_i}{\beta_i H^2}W_{i,\xi} + S_{11A}\frac{1}{\beta_i^3 H^2}W_{i,\xi}W_{i,\xi\xi} = 0 \\
&-\frac{1}{12}S^{(i)}_{11D}\frac{\alpha_i^2}{\beta_i^4}W_{i,\xi\xi\xi\xi} + \Big(\frac{S_{11A}H^2}{\beta_i^3}U_{i,\xi} + \frac{S_{11A}}{2\beta_i^4}W^2_{i,\xi} - \frac{S_{12A}K_i}{\beta_i^2}W_i - \frac{S_{22A}H^2}{\beta_i^2}N^p_{iEx}\Big)W_{i,\xi\xi} + \frac{S_{12A}K_iH^2}{\beta_i}U_{i,\xi} \\
&+\frac{S_{12A}K_i}{2\beta_i^2}W^2_{i,\xi} - S_{22A}K_i^2W_i - S_{22A}H^2K_iN^p_{iEy} + T^{(i)}_c\frac{1}{2}(1+\tanh(AK_H(\mathrm{sign}(W_2-W_3))(|W_2-W_3|)^{3/2})) \\
&\times\frac{H^4}{\alpha_i}K_H(\mathrm{sign}(W_2-W_3))(|W_2-W_3|)^{3/2} + \frac{S_{22A}}{\alpha_i}Q^{(i)} = S_{22A}(1+p_i)W_{i,\tau\tau}
\end{aligned} \tag{48}$$

where $S_{ijA} = A^{(i)}_{ij}/h^{(i)e}, S^{(i)}_{11D} = D^{(i)}_{11}/[(h^{(i)e})^3/12]$.

Assuming the both ends of axisymmetrical piezoelectric laminated cylindrical shell are movably clamped, the dimensionless boundary conditions are

$$\begin{aligned}
&W_1(0) = 0, N_{1\xi}(0) = 0, W_{1,\xi}(0) = 0 \\
&W_4(1) = 0, N_{4\xi}(1) = 0, W_{4,\xi}(1) = 0
\end{aligned} \tag{49}$$

The dimensionless continuity conditions of displacements are

$$\begin{aligned}
&U_2(0) = U_1(1) + \frac{1-\alpha_2}{2\beta_1 H^2}W_{1,\xi}(1), U_3(0) = U_1(1) - \frac{1-\alpha_3}{2\beta_1 H^2}W_{1,\xi}(1) \\
&U_2(1) = U_1(0) + \frac{1-\alpha_2}{2\beta_4 H^2}W_{4,\xi}(0), U_3(1) = U_4(0) - \frac{1-\alpha_3}{2\beta_4 H^2}W_{1,\xi}(0) \\
&W_1(1) = W_2(0) = W_3(0), W_{1,\xi}(1) = W_{2,\xi}(0) = W_{3,\xi}(0) \\
&W_4(0) = W_2(1) = W_3(1), W_{1,\xi}(0) = W_{2,\xi}(1) = W_{3,\xi}(1)
\end{aligned} \tag{50}$$

The dimensionless equilibrium conditions of moments and forces are

$$\begin{aligned}
&N_{1\xi}(1) = N_{2\xi}(0) + N_{3\xi}(0), M_{1\xi}(1) = M_{2\xi}(0) + M_{3\xi}(0) - \frac{1-\alpha_2}{2}N_{2\xi}(0) + \frac{1-\alpha_3}{2}N_{3\xi}(0) \\
&N_{4\xi}(0) = N_{2\xi}(1) + N_{3\xi}(1), M_{4\xi}(0) = M_{2\xi}(1) + M_{3\xi}(1) - \frac{1-\alpha_2}{2}N_{2\xi}(1) + \frac{1-\alpha_3}{2}N_{3\xi}(1)
\end{aligned} \tag{51}$$

The expressions of $N_{i\xi}$ and $M_{i\xi}$ in Eqs. (49) and (51) are

$$N_{i\xi} = S_{11A}\alpha_i\left(\frac{1}{\beta_i}U_{i,\xi} + \frac{1}{2H^2\beta_i^2}W^2_{i,\xi}\right)h^e - S_{12A}\alpha_i\frac{K_i}{H^2}W_i, M_{i\xi} = S^{(i)}_{11D}\left(-\frac{\alpha_i^3}{12\beta_i^2}W_{i,\xi\xi}\right)\frac{(h^e)^3}{L^2} \tag{52}$$

The dimensionless initial conditions are

$$\tau = 0, W_i = W_{i,\tau} = 0 \tag{53}$$

3. Solution methodology

In present study, we take $q^{(1)} = q^{(4)} = q^{(3)} = 0, q^{(2)} = q$ and the transverse load q is taken as

$$q(x,t) = Q\cos x \sin \omega t \tag{54}$$

where Q and ω are the amplitude value and frequency of external load, respectively.

The considered domain of each region is $0 \leqslant \xi_1, \xi_2, \xi_3, \xi_4 \leqslant 1$ and each region is divided into M sections as shown in Fig. 2. The points on dotted line are imaginary points.

Firstly, all partial derivative items related to the space coordinate variable are replaced by difference scheme in disposing of nonlinear governing Eq. (48), boundary conditions (49), continuity conditions (50) and equilibrium conditions of moments and forces (51). The difference schemes of all partial derivative items in these equations as $U_{j,\xi}$, $U_{j,\xi\xi}$, $W_{j,\xi}$, $W_{j,\xi\xi}$, $W_{j,\xi\xi\xi\xi}$ can be easily obtained. Then the nonlinear items of governing equations and corresponding conditions are linearized and can be written as follows:

$$(X \cdot Y)_J = (X)_J (Y)_{J_p} \tag{55}$$

in which $(Y)_{J_p}$ is the value of the former iterative. For the primary iteration, secondary extrapolation method is introduced to obtain the value of $(Y)_{J_p}$, that is

$$(Y)_{J_p} = A(Y)_{J-1} + B(Y)_{J-2} + C(Y)_{J-3} \tag{56}$$

As for different iterations, the coefficients A, B and C are decided as follows:

$$\begin{aligned} &j = 1: \; A = 1, B = 0, C = 0 \\ &j = 2: \; A = 2, B = -1, C = 0 \\ &j \geqslant 3: \; A = 3, B = -3, C = 1 \end{aligned} \tag{57}$$

At the same time, the partial derivative items relative to the time are replaced by Newmark $-\beta$ scheme. The actuation duration τ is divided into n sections, each section is $\Delta\tau = \tau/n$, then $W_{j,\tau\tau}$ at point i can be expressed as

$$(W_{j,\tau\tau})_i^{(n)} = \frac{4[(W_j)_i^{(n)} - (W_j)_i^{(n-1)}]}{(\Delta\tau)^2} - \frac{4(W_{j,\tau})_i^{(n-1)}}{\Delta\tau} - (W_{j,\tau\tau})_i^{(n-1)} \tag{58}$$

where

$$\begin{aligned} &(W_{j,\tau})_i^{(n)} = (W_{j,\tau})_i^{(n-1)} + \frac{1}{2}[(W_{j,\tau\tau})_i^{(n-1)} + (W_{j,\tau\tau})_i^{(n)}]\Delta\tau \\ &(W_j)_i^{(n)} = (W_j)_i^{(n-1)} + (W_{j,\tau})_i^{(n-1)}(\Delta\tau) + \frac{1}{4}[(W_{j,\tau\tau})_i^{(n-1)} + (W_{j,\tau\tau})_i^{(n)}](\Delta\tau)^2 \end{aligned} \tag{59}$$

After the equations and conditions are linearized and disposed by using the finite difference method and Newmark method, the nonlinear partial differential equations are transformed into linear algebraical equations expressed by difference schemes. These algebraic equations are solved by using the iteration method. For every step, the iterative lasts until the difference of the present value and the former is smaller than 0.01%, then continue the calculation of the next step.

Suppose the initial delamination growth rate is equal to zero in the first period of external load. After obtaining U_i, W_i by solving the algebraic equations, the amplitude of energy release rate along the delamination front can be determined by Eqs.

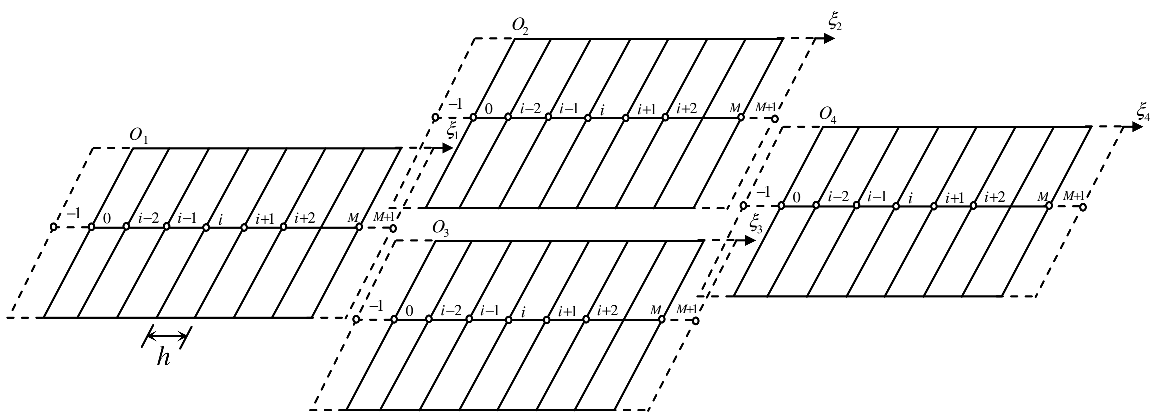

Fig. 2. The dimensionless regions and the finite difference points.

(36), (43) and (45). Then according to Eq. (46), the delamination growth rate of this period can be obtained and the delamination growth length can be calculated. The length of each region is recalculated after delamination growth, then continues the calculation of the next period.

It is impossible to analyze fatigue delamination growth under huge numbers of cyclic loads. In order to save the time, the cyclic skip method is employed, that is, when the calculation process is in the quasi-stable state, the delamination growth rate $(\mathrm{d}a/\mathrm{d}N)_k$ is considered to be constant under a certain segmentation of cyclic loads (the corresponding cyclic number ΔN_k). Then we have

$$\Delta N_k = \frac{(\Delta a)_k}{(\mathrm{d}a/\mathrm{d}N)_k} \tag{60}$$

where $(\Delta a)_k$ is the average delamination growth length under cyclic loads (the corresponding cyclic number ΔN_k). From Eq. (60), the total delamination growth length is

$$a_{k+1} = a_k + \left(\frac{\mathrm{d}a}{\mathrm{d}N}\right)_k \Delta N_k \tag{61}$$

where a_k is the total delamination growth length without applying the cyclic loads (the corresponding cyclic number ΔN_k).

4. Numerical results and discussion

In numerical examples, consider a symmetrically cross-ply $[0^0/90^0/0^0]_{10}$ laminated cylindrical shell. All layers have same thickness and are composed of carbon/epoxy composite, and the material constants are $E_{\mathrm{L}} = 150.0$ GPa, $E_{\mathrm{T}} = 9.0$ GPa, $G_{\mathrm{LT}} = 7.1$ GPa, $\mu_{\mathrm{LT}} = 0.3$, $\rho^{\mathrm{e}} = 2.7 \times 10^3$ kg/m^3. The piezoelectric layers are composed of piezoelectric ceramic PZT-5, and the material constants are $E_{\mathrm{L}} = 62$ GPa, $E_{\mathrm{T}} = 62$ GPa, $G_{\mathrm{LT}} = 23.6$ GPa, $\mu_{\mathrm{LT}} = 0.3$, $\rho^{p} = 7.75 \times 10^3$ kg/m^3, $d_{31} = d_{32} = -220 \times 10^{-12} m/V$. Let the voltage of the upper piezoelectric layer equal to the down layer, that is, $V_{\mathrm{T}} = V_{\mathrm{B}}$. The dimensionless geometric parameters and physical parameters are given as follows:

$$\begin{aligned}
&\alpha_1 = 1, \alpha_2 = 0.2, \alpha_3 = 0.8, \alpha_4 = 1, p_1 = 0.574, p_2 = 0.287, p_3 = 0.287, p_4 = 0.574, \mu = 0.3\\
&Q = 1000, \omega = 1, N^{\mathrm{p}}_{1\mathrm{E}x} = N^{\mathrm{p}}_{4\mathrm{E}x} = N^{\mathrm{p}}_{1\mathrm{E}y} = N^{\mathrm{p}}_{4\mathrm{E}y} = -0.002, N^{\mathrm{p}}_{2\mathrm{E}x} = N^{\mathrm{p}}_{3\mathrm{E}x} = N^{\mathrm{p}}_{2\mathrm{E}y} = N^{\mathrm{p}}_{3\mathrm{E}y} = -0.001\\
&L/R = 5/3, R/h^{\mathrm{e}} = 30, H = 50, K_1 = K_4 = 83.33, K_2 = 83.612, K_3 = 82.237
\end{aligned}$$

For comparison of present results with the literature (Yang et al., 2006), the nonlinear center deflection–time response curves of isotropic cylindrical shells with symmetrical delamination are presented in Fig. 3. Here, $W^0_i (i = 2, 3)$ denotes the dimensionless center deflection of regions 2 and 3, respectively. A good agreement is observed between the corresponding two sets of values. Thereby it is validated that the present analytical method and calculating procedure are reliable.

Figs. 4–11 show the effects of voltages, stiffness factor of contact region, asymmetry of delamination and delamination length on the nonlinear dynamic responses, the energy release rate and the delamination growth length of delaminated piezoelectric laminated cylindrical shell. In all figures, $N^{\mathrm{p}}_{1\mathrm{E}x}$ is the dimensionless additional inner force of piezoelectric layer after applying voltage on it, $N^{\mathrm{p}}_{1\mathrm{E}x}$ is equal to zero when the voltages are not applied, β_1 is the dimensionless distance between the left edge of delamination and the left end of cylindrical shells, β_2 is the dimensionless length of delamination, K_{H} is the stiff-

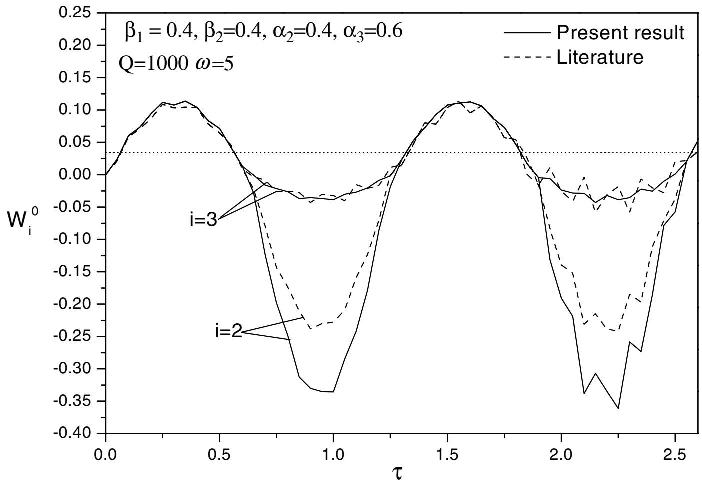

Fig. 3. Comparison of nonlinear deflection–time response curves of regions 2 and 3 for delaminated isotropic cylindrical shell.

ness factor of contact region, and Δa is the fatigue delamination growth length along the delamination front, $N$is the cyclic number.

The effect of contact region stiffness on the nonlinear dynamic response of regions 2 and 3 are shown in Fig. 4. It can be observed that with the decrease of contact region stiffness, the center response amplitude of region 2 increases and the penetration will emerge in the delamination contact region. According to the contact law, large penetration is un-logical. Therefore, proper stiffness factor of contact region needs to be derived by experiments for different material.

The effect of voltages on the nonlinear dynamic response of regions 2 and 3 is shown in Fig. 5. It can be seen that the center response amplitudes of the two regions decrease when positive voltages are applied on piezoelectric layers. It is because that applying positive voltages is equal to applying an additional planar tension on the cylindrical shells.

The effect of contact region stiffness on the energy release rate G on the left edge of delamination is shown in Fig. 6. It can be observed that the maximum energy release rates and the delamination growth rate along the delamination fronts decrease with the increase of contact region stiffness. The reason is that the nonlinear dynamic response amplitude of delamination dramatically decreases in the anterior half-period.

The effect of delamination asymmetry on the energy release rates G on the both edges of delamination is shown in Fig. 7. It can be seen that the maximum energy release rate on the left edge of delamination is larger than the maximum energy release rate on the right edge.

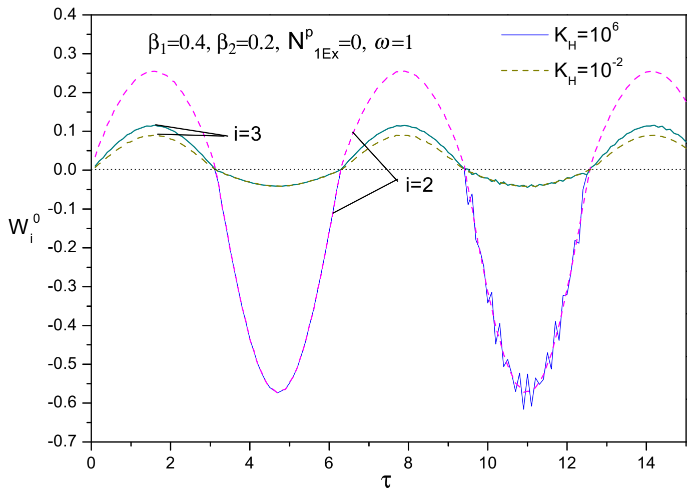

Fig. 4. Effect of contact region stiffness on nonlinear deflection–time response curves of regions 2 and 3 for delaminated piezoelectric laminated cylindrical shell.

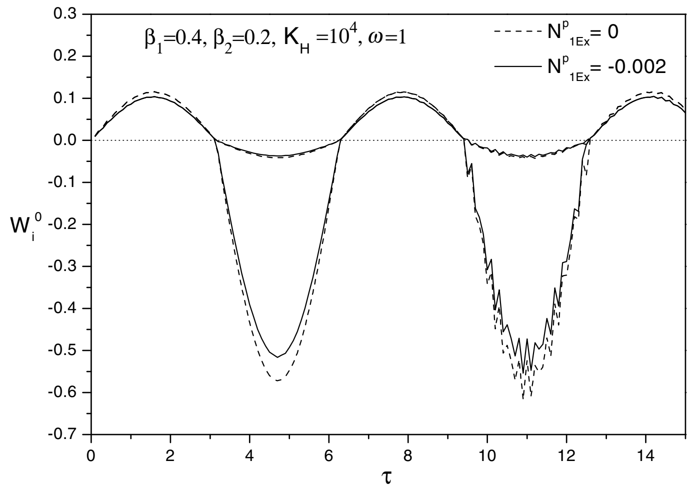

Fig. 5. Effect of voltages on nonlinear deflection–time response curves of regions 2 and 3.

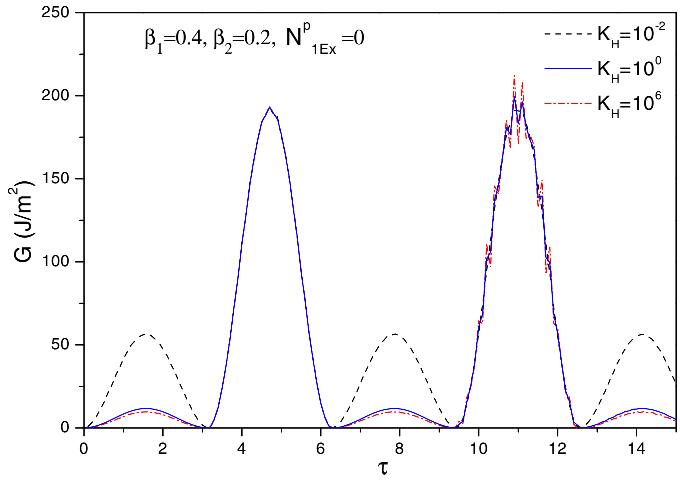

Fig. 6. Effect of contact region stiffness on energy release rates along the delamination front.

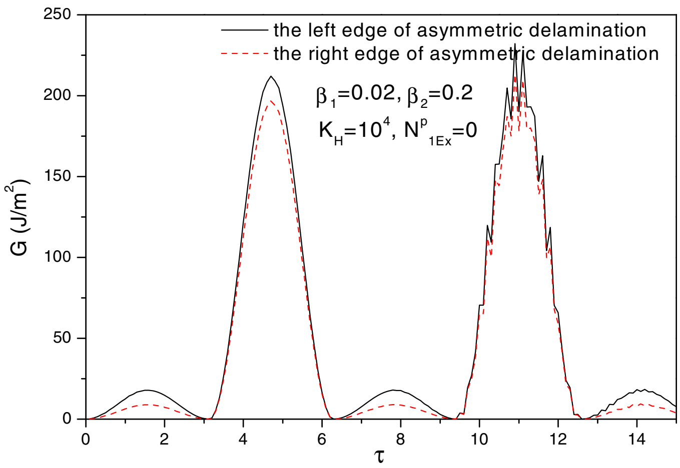

Fig. 7. Effect of delamination asymmetry on response curves of energy release rates with time on the both edges of delamination.

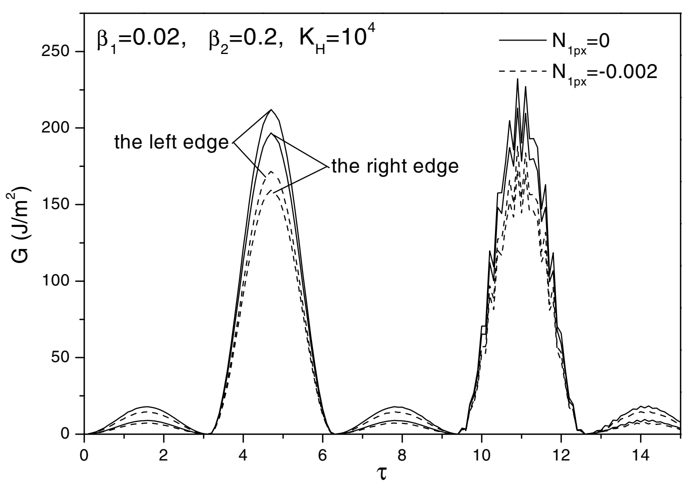

Fig. 8. Effect of voltages on response curves of energy release rates with time on the both edges of asymmetric delamination.

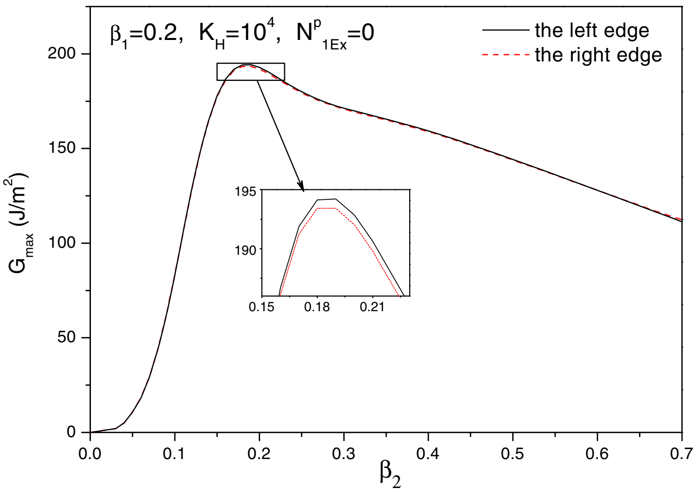

Fig. 9. Effect of delamination length on the maximum energy release rate along the delamination front.

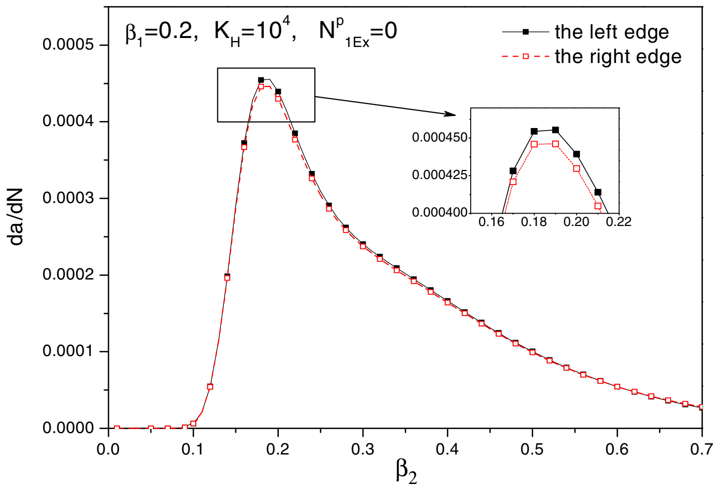

Fig. 10. Effect of delamination length on delamination growth rate.

The effect of voltages on the energy release rate G on the both edges of delamination is shown in Fig. 8. It can be observed that the energy release rates on the both edges of delamination decrease after applying positive voltages.

The effect of the delamination length β_2 on the maximum energy release rate G for piezoelectric laminated cylindrical shell with asymmetric delamination is shown in Fig. 9. It can be seen that the energy release rate reaches the maximum value when $\beta_2 = 0.19$ and it will decrease with the further increase of delamination length. It indicates that the delamination growth of piezoelectric laminated cylindrical shell may be stable.

The effect of the delamination length on the delamination growth rates da/dN for piezoelectric laminated cylindrical shell with asymmetric delamination is shown in Fig. 10. It can be seen that the delamination growth rate on the left edge of delamination is slightly larger than that on the right edge. It is because that the maximum energy release rate is larger on the left edge of delamination.

Taking the length of delamination $\beta_2 = 0.05$, the effect of voltages on the delamination growth length Δa on the both edges are shown in Fig. 11. Comparing Fig. 11(a) with (b), it can be observed that the delamination growth length on the right edge of delamination is 1.5 mm after 2×10^{10} cycle loads when positive voltages are not applied, and that is 0.123 mm after applying voltages. It can be known that the velocity of delamination growth decreases after applying voltages. The reason is that the delamination growth rate decreases after applying positive voltages.

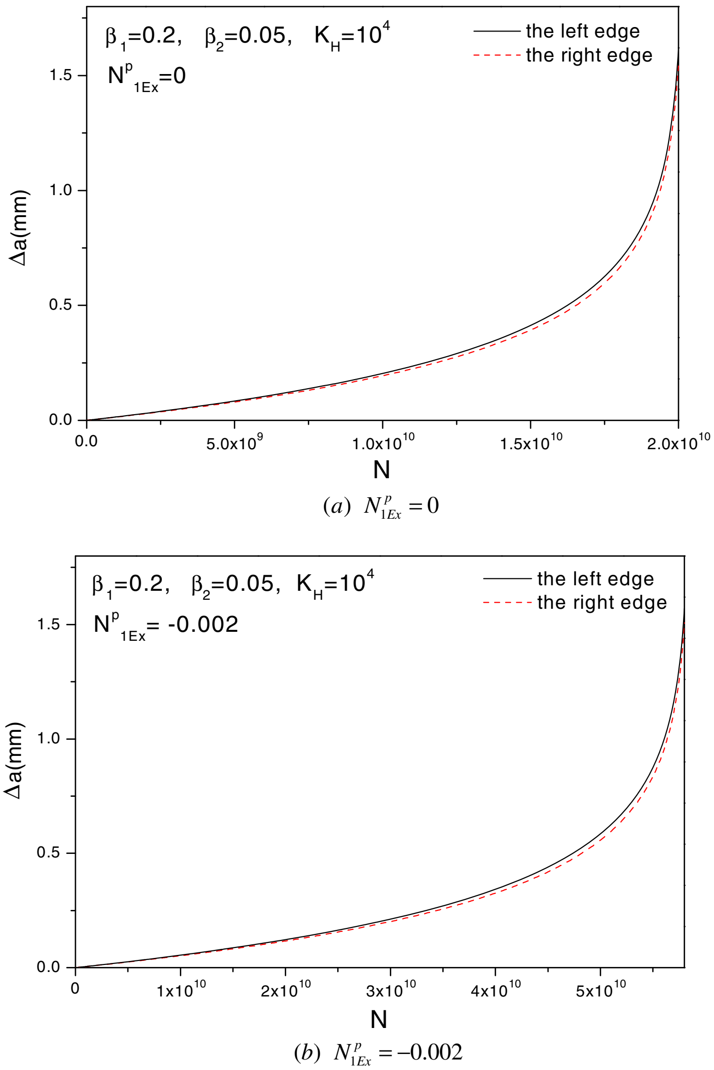

Fig. 11. Effect of voltages on delamination growth length along the delamination front.

5. Conclusions

A nonlinear analysis model of fatigue delamination growth for piezoelectric laminated cylindrical shells with asymmetric laminations is presented. Considering the geometric nonlinearity and the nonlinear contact effect, the nonlinear governing equations and corresponding matching conditions for the delaminated shells are established by using the movable-boundary variational principle. According to the Griffith criterion and Paris law, the energy release rate and delamination growth rate along the delamination front are determined. Then, using cyclic skip method, the delamination growth lengths are derived. Based on the present analysis, some conclusions may be drawn.

After increasing the stiffness of contact region, the emergence of delamination penetration is avoided and the maximum energy release rate dramatically decreases in the anterior half-period. When positive voltages are applied on the piezoelectric layers, the nonlinear dynamic response amplitude and the maximum energy release rates decrease, the growth of delamination slows down. With the increase of delamination length, the delamination growth rate increases in the beginning, however it will decrease rapidly after reaches the maximum value. The energy release rate of the piezoelectric laminated cylindrical shell with asymmetric delamination is larger than that with symmetric delamination.

References

Blanco, N., Gamstedt, E.K., Asp, L.E., et al, 2004. Mixed-mode delamination growth in carbon-fibre composite laminates under cycle loading. International Journal of Solids and Structures 41, 4219–4235.

Chen, H., Wang, M., 2006. The effect of nonlinear contact upon natural frequency of delaminated stiffened composite plate. Composite Structure 76, 28–33.
Chen, Y., 2003. Nonlinear vibration of transversely isotropic piezoelectric rectangular plate. Journal of Nanjing University of Aeronautics & Astronautics 35 (1), 18–24.
Giannakopoulos, A.E., Nillsson, K.F., 1993. Dynamic energy release rate of delaminations based on Mindlin-type nonlinear theory. Journal of Applied Mechanics 60 (4), 1046–1047.
Qian, W.C., 1980. Variational Calculus and Finite Element. Science Press, Beijing. in Chinese.
Schön, J., 2000. A model of fatigue delamination in composites. Composites Science and Technology 60, 553–558.
Shi, G.Y., 2003. Electric enthalpy of piezoelectric materials and coupling analysis of mechanical and electric field. Acta Materiae Composite Sinica 20 (6), 115–120.
Schwarts, H., 2007a. High-order nonlinear contact effects in the dynamic behavior of delaminated sandwich panels with a flexible core. International Journal of Solids and Structures 44, 77–99.
Schwarts, H., 2007b. High-order nonlinear contact effects in cyclic loading of delaminated sandwich panels. Composite: Part B 38, 86–101.
Takeda, N., 1999. Effects of toughened interlaminar layer on fatigue damage progress in quasi-isotropic CFRP laminates. International Journal of Fatigue 21, 235–242.
Wang, J.X., 2002. A study of the vibration of delaminated beams using a nonlinear anti-interpenetration constraint model. Composite Structure 57, 483–488.
Wang, Z., 1993. The present state of studies on interfacial dynamics. Shanghai Mechanics 14 (2), 1–10.
Xu, P., 2000. The numerical analysis of piezoelectric laminated plates and shells. Journal of North China Institute of Technology 21 (3), 243–245.
Yang, J.H., Fu, Y.M., Wang, X.Q., 2007. Variational analysis of delamination growth for composite laminated cylindrical shells under circumferential concentrated load. Composite Science and Technology 67 (3), 541–550.
Yang, J.H., Fu, Y.M., 2006. Delamination growth of laminated composite cylindrical shells. Theoretical and Applied Fracture Mechanics 45 (3), 192–203.
Yang, J.H., Fu, Y.M., Wang, Y., 2006. Analysis of nonlinear dynamic response for axisymmetrical delaminated laminated cylindrical shell under considering the effect of contact. Engineering Mechanics 23 (3), 69–75.
Yin, W.L., 1993. Energy balance and the speed of crack growth in a compressed plate with delamination. International Journal of Solids and Structures 30 (15), 2041–2055.
Zhao, Y.P., 1996. The advances of studies on the dynamic initiation of cracks. Advances in Mechanics 26 (3), 362–378.